Multi-scalar and velocity measurements in a turbulent bluff-body flame using spectral fitting of Spontaneous Raman Scattering and PIV

Florestan Guichard, Nelson Valdez, Pascal Boubert, David Honoré, Corine Lacour, Bertrand Lecordier, Armelle Cessou

Multi-scalar and velocity measurements in a turbulent bluff-body flame using spectral fitting of Spontaneous Raman Scattering and PIV

Florestan GUICHARD, Nelson VALDEZ, Pascal BOUBERT, David HONORE*,
Corine LACOUR, Bertrand LECORDIER, Armelle CESSOU

Normandie Univ, INSA Rouen, UNIROUEN, CNRS, CORIA, 76000 Rouen, France

Abstract

The objective of this study is to experimentally investigate the complex shear and mixing layers of the recirculation zone at the exit of a canonical bluff-body burner by spontaneous Raman scattering and PIV, in order to have a deeper understanding of combustion mechanisms that lead to the stabilization of the flame. Temperature and multi-species number density profiles across the recirculation zone of the bluff-body burner are compared with velocity fields measured by PIV and flame imaging to identify the specific features of the flame in the recirculation zone consisting in eddies of partially burnt gas and a diffusion flame of CO close to the annular air flow.

Introduction

Depletion of fossil fuels and environmental issues make necessary an in-depth study of combustion processes to improve the energy efficiency and adaptability of industrial burners. Bluff-body burners are widely used to ensure stabilization of large turbulent non-premixed flames in many industrial applications, such as gas turbines, ramjets and furnaces [1, 2]. The internal recirculation zone generated by the wake effect of the flows downstream of the bluff-body consists of one central jet driven centrifugal vortex and one outer air driven centripetal vortex [3, 4]. Such complex flow induces then the partially mixing of the fuel with oxidant as well as the trapping of high-temperature combustion products which brings the necessary heat for the stabilization of the flame [5-7].

The objective of this study is to experimentally investigate the complex shear and mixing layers in the recirculation zone at the exit of a canonical bluff-body burner by spontaneous Raman scattering and PIV, in order to have a deeper understanding of combustion mechanisms that lead to the stabilization of the flame.

Simultaneous temperature and multi-species density numbers from Spontaneous Raman Scattering (SRS) measurements provide valuable information to describe such turbulent flames. However, in the case of highly turbulent and locally rich hydrocarbon flames, single-shot SRS measurements require powerful excitation system and sensitive detection setup with short exposure time because of the low cross-section of SRS compared to the strong radiation from the flame. 1D single-shot SRS measurements with 330 µm spatial resolution are collected in the core of the recirculation zone, for several radial positions to get a complete profile of about 30 mm, from the methane central jet to the ambient air. Quantitative number densities for all major species (N_2, O_2, CO, CO_2, H_2O and CH_4) are extracted simultaneously from single-shot spectra using a spectral fitting method. Temperature of the probe volume is obtained from the minimization of synthetic spectra of N_2 with the experimental ones. In the fuel jet where nitrogen is absent or in too low concentration, temperature is extracted up to 1500 K from spectral fitting of methane SRS. In rich and luminous regions of the flame, strong interferences from C_2 emission on N_2 and CO Raman scattering spectra are rigorously removed by spectral fitting of the Swan bands. With this original method, instantaneous temperature and multi-species concentrations can be measured in the overall mixture fraction frame, in lean, rich, luminous and slightly sooty region of a turbulent flame, what is challenging for SRS.

In the present work, temperature and multi-species number densities profiles across the recirculation zone of the bluff-body burner are compared with velocity measured by PIV and flame imaging results to identify and characterize precisely all the specific features of the flame in the recirculation zone consisting in eddies of partially burnt gas and a diffusion flame of CO close to the annular air flow. These results highlight the leading role of the aerodynamics of the recirculation zone close to the burner exit in the stability of such complex turbulent flame.

The Bluff-Body burner

The flame investigated is stabilized downstream to a non-premixed bluff-body burner consisting of two coaxial jets. The experimental device is presented in Figure 1. Methane is injected in the central jet (D_j = 7.5 mm) while air is injected in the annular flow (D_a = 55 mm). The D_b = 48 mm-dia. bluff-body induces a large blocking ratio of 0.83.

The chosen operating conditions (labeled F1 flame in [8]) - with central methane jet velocity Uj = 10.5 m/s and annular air velocity Ua = 5 m/s - lead to a typical turbulent Bluff-Body flame stabilized in the recirculation zone generated in the vicinity of the burner exit (Figure 2).

* Corresponding author: david.honore@coria.fr

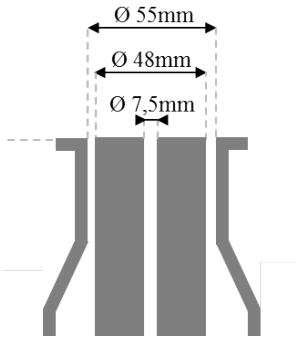

Figure 1: The non-premixed Bluff-Body burner

Figure 2: Photograph of the turbulent Bluff-Body flame

The flame structure and velocity fields are obtained by fast OH* chemiluminescence imaging and fast PIV. The set-up and the results are presented in details in [8]. The 7500-singleshot average velocity field obtained for F1 flame is presented in Figure 3.

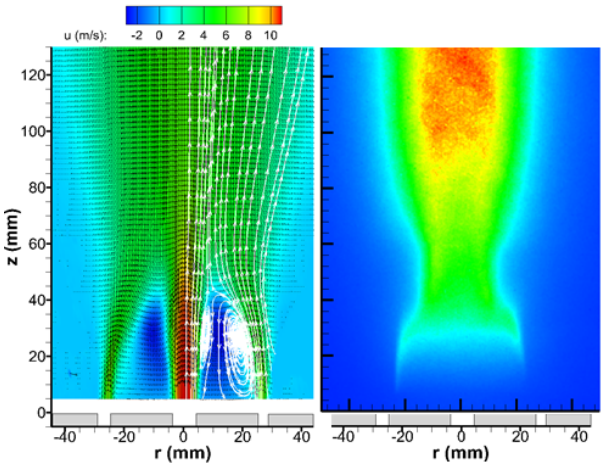

Figure 3: 7500-singleshot averaged velocity fields with superimposed streamlines (left) and OH chemiluminescence average image (right).*

From the burner exit, the mean reaction zone is located at the external border of the recirculation zone. Downstream in the flow, a mean jet-like flame is developed in continuity. The average flame image does not illustrate the unsteadiness of the turbulent flow and the intermittent flame, which is detailed in [8].

Spontaneous Raman scattering

The weakness of the SRS efficiency requires a specific experimental set-up to provide signal-to-noise ratio suitable for single-shot measurements with a high spatial resolution. The laser source consists in a Nd:YAG laser (Agilite Continuum) operating at 10 Hz providing up to 1.8 J with top-hat pulse with a long pulse duration adjustable from 200 ns till 1 µs, to obtain good spatial resolution without any optical breakdown. In the purpose of investigating flames of hydrocarbon fuels, a green laser is chosen to avoid of inducing fluorescence while higher signal are expected with UV laser [9]. The laser beam is focused using a convergent lens with a 1 m focal-length providing a probe volume of 170 µm- thick ($1/e^2$). The SRS light is collected at 90° with a large solid angle (f/2) using two telescopes composed of achromatic lenses. The scattered light at the laser wavelength is suppressed by a notch filter (NF03-532E, Semrock, OD = 6 at 532 nm, FWHM = 17 nm, transmission efficiency in passbands > 93%) placed in the second collimated part of the optical collection system. Then, a periscope is used to rotate the image of the laser beam parallel to the entrance slit of the spectrograph. The single-shot spectra of SRS are acquired with a spectrograph IsoPlane SCT 320 (Princeton Instruments) equipped with a grating of 600 grooves/mm and providing a spectral resolution of 0.67 nm.

The detector camera is a full-frame back-illuminated CCD (Pixis 400B, Princeton Instruments, 1340 x 400 pixels, pixel size 20 µm, NF = 1). This camera offers approximately 94 % of QE with 16-bits of dynamic range and readout noise (< 13 e-). The line-wise measurements are performed by imaging almost 3 mm of laser beam. For single-shot measurements along this length, 8 local probe volumes of 50 pixels height each are selected by dividing the image of the laser beam with hardware binning, resulting in 8 simultaneous probe volumes and a spatial resolution of 330 µm.

The collection is gated by a fast electro-optical shutter composed of a Pockels Cell Shutter (PCS) [10] to limit the flame emission background. With the PCS switched on, the flame emission is integrated during a small time interval (500 ns or 1 µs) chosen to fit the laser pulse duration making the contribution of the flame emission to the spectra negligible. Behind the PCS, an achromatic half-wave plate (AHWP10M-600, Thorlabs) is placed in front of the spectrograph and oriented in order to obtain the best efficiency of the spectrograph.

Instantaneous 1D radial measurements are collected from z = 12 mm to 90 mm above the burner. The 12 mm profile crossing the recirculation zone at the minimum flame height is selected in the present paper. 8 simultaneous measurements along 3 mm are collected with spatial resolution of 330 µm. The complete radial profile is built along 30 mm by shifting the burner thanks to a motorized bench. At z = 12 mm, the burner does not mask the collection solid angle keeping f/2 collection aperture. 600 instantaneous acquisitions are recorded at each radial location.

Instantaneous thermometry and concentration measurements by spectral fitting

Local instantaneous temperature is determined by the procedure proposed by Lo et al [11] where the theoretical spectra are convoluted with apparatus functions determined from SRS radiation collected in-situ and automatically least-square fitted to the experimental spectra. The accuracy of the temperature

determination depends on the noise level and on the fidelity of the apparatus function, which affects the shape of the spectrum and the spectral resolution and varies along the probe volume. The determination of an apparatus function at each probe volume [11] leads to a high accuracy of the temperature measurement along the probed distance, despite its change due to the short focal length of the collection lens and the moderate length of the spectrograph. The procedure has been first assessed for N_2 and more generally diatomic molecules, and has shown all its interest especially in its ability to quantify the vibrational non-equilibrium in discharge [11]. The method has been extended to polyatomic spectra, CO_2, H_2O and recently CH_4.

Carbon dioxide SRS spectra are modeled using a table recently released by [12] and specifically designed for combustion diagnostic. Their work is based on an original algebraic approach to keep a connection with configuration space and describe the CO_2 behavior with either local or normal coordinates. Finally, their simulation of a high resolution CO_2 spectrum in burnt gases shows results very close to experimental accuracy [13]. The minimization procedure carried out on the full CO_2 SRS spectra, lead to a systematic overestimation of the temperature in hot burnt gases. Thus new borders for the minimization are fixed to reduce the influence of the CO_2 ro-vibrational wings, which are not correctly modeled by the spectroscopic database. The adapted procedure leads to a correct modeling of the spectra, providing accurate temperature measurement overall the flame temperature range [14], and used here for CO_2 concentration measurements,

For water vapor concentrations measurements, the spectrum modeling included in the Raman Code is based on the H_2O transition table developed by Avila et al. for combustion [15, 16]. Available since 2004, this table including more than 120 000 rotation-vibration transitions between 3100 cm^{-1} and 4300 cm^{-1} and taking into account rotation and vibration levels up to 13 000 cm^{-1} is suitable up to at least 2000 K [17].

Methane modeling is based on a transitions table build by Badr Amyay from Institut Carnot of Bourgogne, developed from absorption spectra of CH_4 present in exoplanet atmosphere [18, 19]. This table is specifically for modeling up to 1450 K, including the cold band $P_0 \rightarrow P_2$ (28 757 transitions), and the two hot bands $P_1 \rightarrow P_3$ (383 950 transitions) and $P_2 \rightarrow P_4$ (3 313 142 transitions). Due to the very high number of transitions (more than 3 millions), only the 600 000 more intense lines required to carry out 99.5% of the total cross-section at 1450K are kept. Thanks to these data, temperature is extracted up to 1500 K from spectral fitting of methane SRS when nitrogen is absent or in too low concentration.

In rich flames or diffusion flames, where polycyclic aromatic hydrocarbons (PAH) can be present, the quantification of Raman scattering signal can be altered by LIF interferences [9], in particular C_2 LIF produced by photolysis of PAH [20] when 532 nm excitation wavelength is used. Figure 4 shows an example of a SRS spectrum presenting C_2 interferences measured in the recirculation zone of the bluff-body methane-air non-premixed flame. An usual method to remove these LIF interferences is to collect the two cross polarization components of light and to subtract the two spectra to get a spectrum free of the non-polarized lights and keeping only the rovibrational Raman bands. However in turbulent flames, the two polarization components have to be collected simultaneously, imposing to double the collection system [21-23]. To avoid this delicate experimental method, C_2 LIF spectra are fitted with home-made theoretical spectra by the same minimization process used for Raman spectra. The spectra are minimized in the spectral range 555 – 565 nm, on the vibrational band $\Delta v = -1$ of the ($d^3\Pi \rightarrow a^3\Pi$) electronic transition. Then the spectra are calculated over the complete spectral range with the temperature determined from the previous minimization. Figure 4 shows the good agreement of the modeled spectra within the 608 – 620 nm range over the extrapolated spectral range from 565 to 680 nm. Thus, the subtraction of the complete C_2 LIF spectrum on experimental spectra allows to remove this interference and to isolate N_2 and CO SRS spectra (Figure 5).

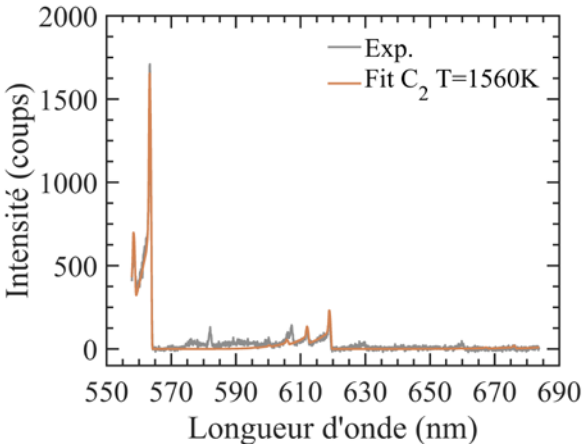

Figure 4: modeling of C_2 LIF emission at the temperature obtained from the fitting performed between 555 and 565 nm (red) superimposed on the experimental SRS spectrum (black)

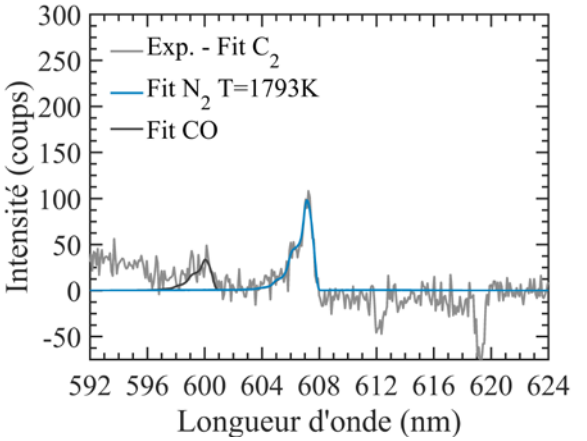

Figure 5: modeling of the N_2 and CO SRS spectra performed after the subtraction of the C_2 LIF interference

Instantaneous concentrations measurements of main reactants, inert gas, and burnt species allow to deduce local instantaneous mixture fraction Z that gives additional information on mixing features of the turbulent non-premixed flame.

Results and discussions

In the central methane jet and its mixing layer, N_2 is absent or in too low concentration for an accurate temperature measurement. In this region, the temperature is determined from the spectral fitting of CH_4 SRS as previously described. Figure 6 shows the superimposed average temperature profiles obtained in the core of the methane central jet and its mixing layer from respectively CH_4 spectra alone (r < 3 mm), from both CH_4 and N_2 spectra (r between 3 and 4.5 mm), and from N_2 alone (r between 4.5 and 7.5 mm). The continuity between all the profiles is excellent. In the potential core, at low temperature and high CH_4 mole fraction, the uncertainty is very low. In the mixing layer, where the signal-to-noise ratio of the two species is enough for an accurate measurement, the fluctuations of the measurements are linked to the mixing layer turbulence, and are equal for CH_4 and N_2.

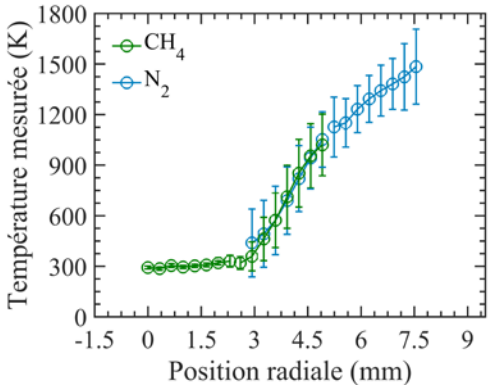

Figure 6: radial profiles of temperature obtained by spectral fittings of CH_4 and N_2 SRS spectra

Aerodynamics of the flow involved in the recirculation zone is complex as illustrated by the streamlines in Figure 3, and is associated to high intermittent unsteadiness of the flame [7]. The flame is blocked in the recirculation zone and is stabilized in the region where the SRS measurement is performed (z = 12 mm). From the velocity field and streamline map, this initial region of the jet can be divided in four radial zones:

Region A [0;4] mm: central methane jet

Region B]4;14] mm: upstream mixing layer

Region C]14 ;22] mm : downstream recirculating burnt gases

Region D]22;30] mm: annular air jet

These regions are presented in Figure 7 along with the mean axial and radial velocity profiles obtained by PIV.

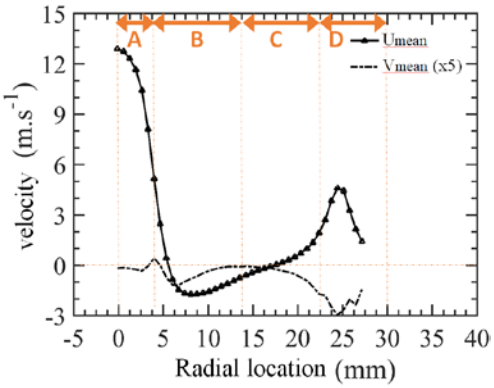

Figure 7: mean axial and radial velocity profiles at z = 12 mm, with definition of the four regions of analysis

Figure 8 shows the 600-single-shot average profiles of temperature and major species mole fraction obtained by SRS.

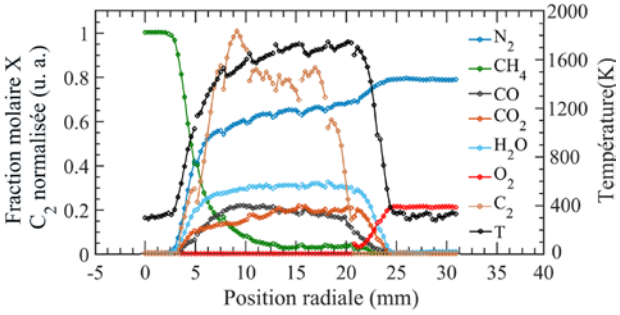

Figure 8: average profiles of temperature and major species mole fraction at z = 12 mm. CO_2, H_2O and CO mole fractions are multiplied by 2.

The mean radial temperature profile shows a hot recirculation zone on either side of the central methane jet and the surrounding annular air flow.

Methane mole fraction equals to 1 in the potential core of the central jet, for r < 2 mm. Farther radially, the CH_4 mole fraction decreases to reach very small, but not zero, mole fraction. The 3D graph, presenting mole fraction versus the radial position r and the mixture fraction Z, shows that in the core of the recirculation zone - between 12 and 25 mm radial positions - methane is still present at very low level but with high fluctuations (Figure 9).

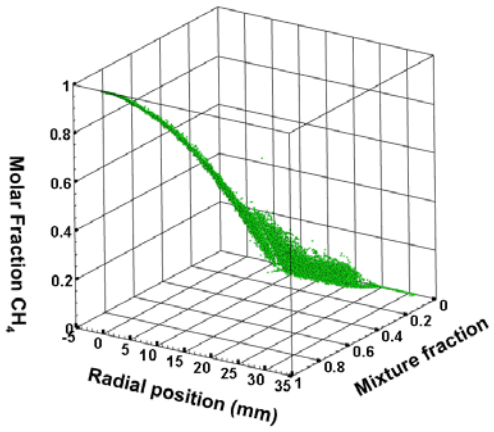

Figure 9: 3D plot of CH_4 mole fraction versus radial location and mixture fraction.

Nitrogen and oxygen profiles show the mixing of the annular air jet from r > 25 mm towards r = 20 mm. From this radial position, O_2 seems to be totally consumed (Figure 8). In fact, the 3D graph in Figure 10, shows that the instantaneous oxygen molar fraction, even if very low (average value close to zero) shows high fluctuation levels within the recirculation zone (10 < r < 22 mm). The mixing line of O_2 is clear between 25 and 22 mm, to reach zero at Z around 0.055, stoichiometric value of CH_4-air mixture.

CO_2 and H_2O profiles show the presence of these two main burnt gas species in the recirculation zone, with molar fractions values of 0.16 and 0.10 for H_2O and CO_2 respectively. Both decrease from the plateaus to zero between r = 22 and 25 mm (Figure 8).

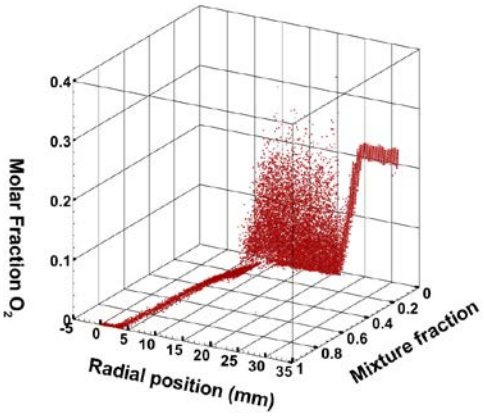

Figure 10: 3D plot of O_2 mole fraction versus radial location and mixture fraction

CO is also present with quite high concentration value, around 0.09, in the recirculation zone. Its concentration decreases as soon as 20 mm, to reach zero at 24 mm. In this region, the CO and O_2 profiles show the combustion of carbon monoxide with the oxygen present in the inner mixing layer of the air annular flow.
The temperature profile in the mixture fraction frame show that a premixed combustion occurs at Z=0.05 (Figure 11). The same observation can be made for all major species mole fraction in the mixture fraction frame.

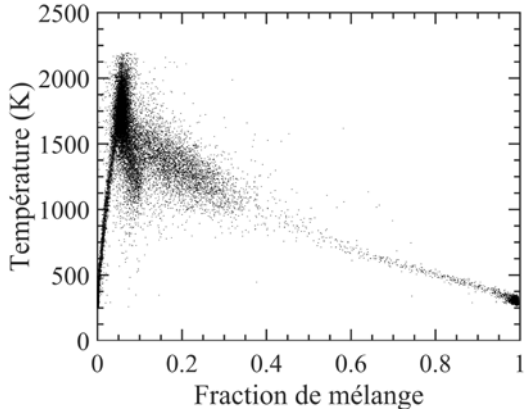

Figure 11: temperature versus mixture fraction at z = 12 mm

This combustion at an almost constant value of mixture fraction (around Z = 0.055) is representative of a premixed combustion, that extends over the whole core of the recirculation zone between r = 5 and 20 mm (Figure 12).

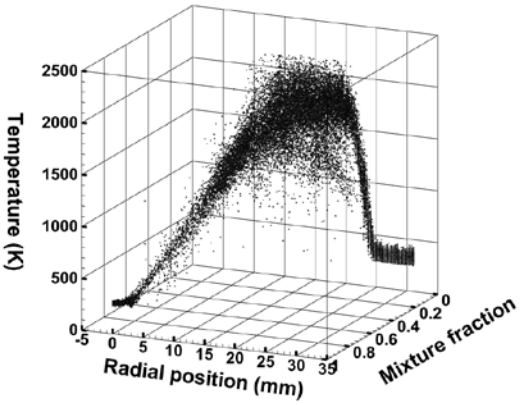

Figure 12: 3D plot of temperature versus radial location and mixture fraction

The comparison of the temperature and the multispecies profiles with the velocity field measurements show the complex mixing through the recirculation zone in the region where the flame is anchored.
Region A: the CH_4 flows from the central jet, the axial velocity is positive with a maximum centerline value of 13 m/s. The limit is given by the peak of radial velocity.
Region B: air engulfed into the recirculation zone goes down in the inner side of the centripetal vortex along the CH_4 jet, mixing with hot burnt gas trapped within the recirculation zone.
Region C: fuel, oxidizer and burnt gas recirculate downstream together in the outer part of the large eddy. In this high temperature region (T > 1500 K), the mixture fraction is almost constant, mostly around the stoichiometric value or slightly rich. The fluctuations of temperature and all species concentrations are high.
Region D: the recirculating gas is entrained into the external air flow. The residual CO in the recirculation zone burns within this mixing layer. The corresponding moving flame can be observed with high speed chemiluminescence imaging (Figure 13).

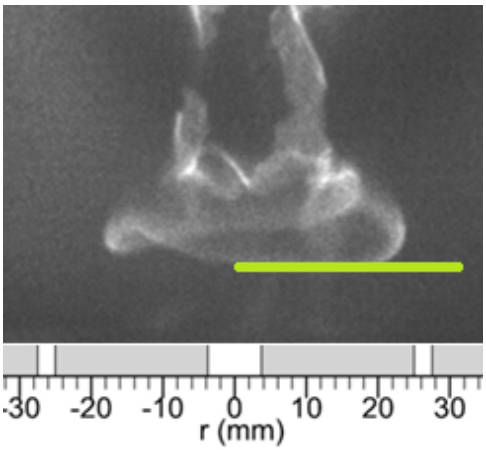

Figure 13: example of instantaneous image of high rate flame chemiluminescence, where the moving flame is observed in the recirculation zone (green line represents the radial profile of SRS measurements).

Conclusions

These first results show that combined analysis of PIV and SRS measurements is useful to describe the complexity of flow and mixing in the recirculation zone of a bluff-body burner. These data will be completed by the map of combined data from 12 to 90 mm downstream to the burner exit. The temperature and multi-species concentration are performed by SRS, with a specific procedure based on spectral fitting to determine temperature from N_2 or CH_4 spectra and concentration of all the major species. The proposed procedure allows to solve the cross-talk between Raman spectra (CO_2-O_2, or CO-N_2) and C_2 LIF spectra with CO and N_2. These measurements are performed in a slightly sooty region (Figure 2), showing that this procedure is a convenient alternative to the Rayleigh based method [24, 25].

Acknowledgements

This work is funded by the BIOENGINE project, co-financed by the European Union with the European regional development fund (ERDF) and by the Normandy Regional Council. This work is also supported by the PASTEC project with the financial support of the French National Research Agency (ANR-16-CE22-0005-02). The PhD fellowship of F. Guichard is supported by Normandy Regional Council.

References

[1] Beér JM, Chigier NA, Combustion Aerodynamics, Applied Science Publishers Ltd, (1972).

[2] Tong, Y., Liu, X., Wang, Z., Richter, M., Klingmann, J, Experimental and numerical study on bluff-body and swirl stabilized diffusion flames, Fuel 217 (2018) 352–364.

[3] Caetano, N. R., Silva, L. F., A comparative experimental study of turbulent non premixed flames stabilized by a bluff-body burner, Experimental Thermal and Fluid Science 63, (2015) 20-33.

[4] A.R. Masri, R.W. Bilger, Turbulent diffusion flames of hydrocarbon fuels stabilized on a bluff body, Symp. (Int.) Combust. 20 (1985) 319.

[5] Susset, K. Mokaddem, D.W. Kendrick, J.C. Rolon, D. Jaffré, D. Honoré, M. Perrin, C. Gray, J.B. Richon, Convenient laser diagnostics for aerodynamic and chemical study of axisymetric non-premixed Bluff-Body burner flames. In: Developments in Laser Techniques and Fluid Mechanics. Selected Papers from the 8th International Symposium Lisbon, 1997.

[6] Susset, M. Trinité, D. Honoré, D. Jaffré, M. Perrin. Experimental investigation of spatio-temporal correlation between aerodynamic and flame front location in an axisymetric non premixed bluff body burner flame. Ninth Int. Symposium on Applications of Laser Techniques to Fluid Mechanics. July 13th-16th, Lisbon, Portugal, 1998.

[7] Mokaddem K., Contribution à la validation expérimentale de deux modèles de combustion turbulente, Ecole Centrale de Paris, 1997 Ph.D. Thesis.

[8] Valdez N., Honoré D., Lacour C., Lecordier B., Cessou A., Turbulent bluff-body flames close to stability limits revealed by coupling of high speed optical diagnostics, 9th European combustion Meeting, ECM 2019, Lisbon, Portugal, 2019.

[9] W. Meier, O. Keck, Laser Raman Scattering in Fuel-Rich Flames: Background Levels at Different Excitation Wavelengths, Meas. Sci. Technol. 13 (2002) 741-749.

[10] H. Ajrouche, A. Lo, P. Vervisch, A. Cessou, Assessment of a fast electro-optical shutter for 1D spontaneous Raman scattering in flames, Measurement Science and Technology 26 (2015) 075501.

[11] A. Lo, G. Cléon, P. Vervisch, A. Cessou, Spontaneous Raman scattering: a useful tool for investigating the afterglow of nanosecond scale discharges in air, Applied Physics B: Lasers and Optics 107 (2012) 229-242.

[12] R. Lemus, M. Sánchez-Castellanos, F. Pérez-Bernal, J.M. Fernández, M. Carvajal, Simulation of the Raman spectra of CO2: Bridging the gap between algebraic models and experimental spectra, J. Chem. Phys. 141 (2014) 1-14.

[13] J.M. Fernandez, A. Punge, G. Tejeda, S. Montero, Quantitative diagnostics of a methane/air mini-flame by Raman spectroscopy, J. Raman Spectrosc. 37 (2006) 175-182.

[14] F. Guichard, Boubert P., Honoré D., Cessou A., CO_2 Spontaneous Raman Scattering: an alternative thermometry for turbulent reactive flows, 19th International Symposium on the Application of Laser and Imaging Techniques to Fluid Mechanics, Lisbon, Portugal, 2018.

[15] G. Avila, J.M. Fernandez, G. Tejeda, S. Montero, The Raman spectra and cross-sections of H_2O, D_2O, and HDO in the OH/OD stretching regions, Journal of Molecular Spectroscopy 228, 38-65, (2004).

[16] G. Avila, J.M. Fernandez, B. Mate, G. Tejeda, S. Montero, Ro-vibrational Raman Cross Sections of Water Vapor in the OH Stretching Region, Journal of Molecular Spectroscopy 196, 77–92, (1999).

[17] J. Tennyson, N.F. Zobov, R. Williamson, O.L. Polyansky, P.F. Bernath, Experimental Energy Levels of the Water Molecule, Journal of Physical and Chemical Reference Data 30, 735, (2001).

[18] B. Amyay, V. Boudon, Vibration-Rotation energy levels and corresponding eigenfunctions of $12CH_4$ up to the tetradecad, Journal of Quantitative Spectroscopy \& Radiative Transfer, 219, 85-104, (2018).

[19] B. Amyay, A. Gardez, R. Georges, L. Biennier, J.V. Auwera, New investigation of the v3 CH stretching region of $12CH_4$ through the analysis of high temperature infrared emission spectra, The Journal of Chemical Physics 148, 134306, (2018).

[20] R.W. Dibble, A.R. Masri, R.W. Bilger, The spontaneous Raman scattering technique applied to nonpremixed flames of methane, Combust. Flame 67 (1987) 189-206.

[21] J. Egermann, W. Koebcke, W. Ipp, A. Leipertz, Investigation of the Mixture Formation inside a Gasoline Direct Injection Engine by Means of Linear Raman Spectroscopy, Proceeding of the Combustion Institute 28 (2000) 1145-1152.

[22] G. Cléon, A. Cessou, D. Stepowski. A new single-shot set-up by spontaneous Raman scattering in turbulent flames. European combustion Meeting, ECM 2007; April 11-13 2007; Chania, Crete, Greece.

[23] G. Magnotti, D. Geyer, R.S. Barlow, Interference free spontaneous Raman spectroscopy for measurements in rich hydrocarbon flames, Proc. Comb. Inst. 35 (2015) 3765-3772.

[24] R.S. Barlow, Laser diagnostics and their interplay with computations to understand turbulent combustion, Proc. Comb. Inst. 31 (2007) 49-75.

[25] F. Fuest, R.S. Barlow, J.-Y. Chen, A. Dreizler, Raman/Rayleigh scattering and CO-LIF measurements in laminar and turbulent jet flames of dimethyl ether, Combust. Flame 159 (2012) 2533-2562.